

# Solid State Characterization of Mometasone Furoate Anhydrous and Monohydrate Forms

XIAOMING (SEAN) CHEN,<sup>1</sup> MATTHEW CARILLO,<sup>1</sup> R. CURTIS HALTIWANGER,<sup>2</sup> PRUDENCE BRADLEY<sup>1</sup>

<sup>1</sup>Discovery Support and Pharmaceutical Chemistry, Pharmaceutical Development, K-11-2 J-4, Schering-Plough Research Institute, Kenilworth, New Jersey 07090

<sup>2</sup>Bruker-AXS, 5465 Cheryl Parkway, Madison, Wisconsin 53711-5373

Received 5 January 2005; revised 21 July 2005; accepted 25 July 2005

Published online in Wiley InterScience (www.interscience.wiley.com). DOI 10.1002/jps.20470

**ABSTRACT:** Mometasone furoate is a potent glucocorticoid anti-inflammatory agent. Its anhydrous Form 1 and monohydrate form were characterized by X-ray crystallography, X-ray powder diffraction at ambient and elevated temperature, thermal analysis, FT-IR, and dynamic moisture adsorption. In Form 1, mometasone furoate molecules pack tightly with molecules interlocked in a space group of  $P2_12_12_1$ . The monohydrate form crystallizes in space group  $P1$ . The unit cell of the monohydrate contains one water molecule and one mometasone furoate molecule. The water molecules form channels along the  $a$  axis and mometasone furoate molecules pack in layers in the same direction. Dehydration was observed between 60 and 100°C by thermogravimetric analysis with a heating rate of 10°C/min. It corresponds to a broad endotherm over the same temperature range in the differential scanning calorimetry with the same heating rate. Variable temperature X-ray powder diffraction reveals that a new anhydrous form (Form 2) was fully produced above 90°C. This crystalline form was converted to Form 1 after being heated above 150°C; and was totally converted to the monohydrate after 1 day at 23°C, 45% RH. © 2005 Wiley-Liss, Inc. and the American Pharmacists Association *J Pharm Sci* 94:2496–2509, 2005

**Keywords:** mometasone furoate; anhydrous form; monohydrate; crystal structure; solid state; physical characterization; hydration

## INTRODUCTION

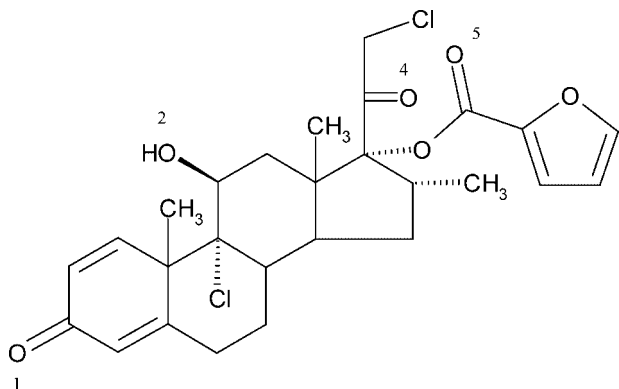
Mometasone furoate (MF, SCH 32088, Scheme 1), 9 $\alpha$ , 21-dichloro-11 $\beta$ , 17 $\alpha$ -dihydroxy-16 $\alpha$ -methylpregna-1,4-diene-3,20-dione 17-(2-furoate),<sup>1</sup> is a glucocorticoid anti-inflammatory agent discovered at Schering-Plough. It has very potent anti-inflammatory activity with rapid onset of action.<sup>2</sup> Moreover, it has low systemic absorption. Mometasone furoate is marketed as topical formulations of ointments, creams, and lotions (Elocon).<sup>3</sup> Its aqueous intranasal spray, Nasonex, is one of

the major products used to treat seasonal and perennial allergic rhinitis.<sup>4,5</sup> It has also been developed as a drug powder inhaler (Asmanex) for therapy in the control and management of mild, moderate, or severe persistent asthma in patients 12 years of age and older, and is approved in the European Union and United States.<sup>6</sup>

Even though mometasone furoate has been widely pursued for treatments of respiratory and allergy disease, there is no published report on the solid state characterization of its crystalline forms. It is well accepted that polymorphism and pseudopolymorphism (formation of solvate and hydrate) of molecular solids affect important physicochemical properties such as stability, solubility, dissolution rate, hygroscopicity, and compactibility.<sup>7</sup> Solid state characterization of the physical forms of a drug is critical for selection and

Correspondence to: Xiaoming (Sean) Chen (Telephone: 908-740-5231; Fax: 908-740-2802; E-mail: xiaoming.chen@spcorp.com)

*Journal of Pharmaceutical Sciences*, Vol. 94, 2496–2509 (2005)  
© 2005 Wiley-Liss, Inc. and the American Pharmacists Association



**Scheme 1.** Chemical structure of mometasone furoate. Numbering of oxygen atoms for its crystal structure is listed.

manufacture of appropriate crystal forms for development. It is also necessary for the rational design and development of dosage forms. Mometasone furoate anhydrous Form 1 is easily prepared from organic solvents. Preparation and formulation of its monohydrate form has been patented in 1992.<sup>8</sup> We report the crystal structure of mometasone furoate anhydrous Form 1 and its monohydrate form. Both forms have been characterized using X-ray powder diffraction, thermal analysis, FT-IR and dynamic moisture adsorption. The phase transition of the monohydrate during dehydration has been investigated.

## EXPERIMENTAL

### Material

Micronized mometasone furoate Form 1 is obtained from Schering-Plough (Kenilworth, NJ). A batch of Form 1 with larger particle size was prepared by dissolving the micronized material in 1:1 (v/v) methanol/acetone (30 mg/mL) and mixing with 6 times the volume of hexane. After stirring for 30 min, the solid was harvested using filtration. The mometasone furoate monohydrate form was prepared by dissolving mometasone furoate in acetone (5 mg/mL) and mixing with an equal volume of water. After stirring for 5 h at room temperature, the monohydrate form was harvested using filtration. A batch of monohydrate with reduced particle size was prepared by gently grinding the crystallization batch with a mortar and pestle.

### Single Crystal X-Ray Analysis

A single crystal of mometasone furoate Form 1 was obtained via vapor diffusion using ethanol as

the solvent and hexane as the anti-solvent. Single crystals of its monohydrate were prepared via vapor diffusion using acetone as the solvent and water as the anti-solvent. Preliminary examination and data collection were performed on a Bruker AXS Smart Apex diffractometer (Bruker AXS, Madison, WI) at 296(2) K with graphite-monochromated MoK $\alpha$ -radiation ( $\lambda = 0.71073$ ) controlled with SMART software. Data integration was carried out using the SAINT (SAINTPLUS, Bruker AXS) software package. The structure was solved by direct methods and refined using SHELXTL (Bruker AXS). Nonhydrogen atoms were refined anisotropically. Hydrogen atoms were calculated and placed in idealized positions with isotropic thermal parameters. Table 1 lists the experimental details of the X-ray analysis. The thermal ellipsoid drawing is presented by Ortep-3 for Windows (University of Glasgow, UK). The structure visualization and powder pattern calculation were performed using Accelrys MS Modeling 3.0.1 (Accelrys, San Diego, CA).

### X-Ray Powder Diffraction

X-ray powder diffraction patterns were collected on a Rigaku Miniflex diffractometer equipped with a CuK $\alpha$  radiation ( $\lambda = 1.54056$ ) at 30 mA and 40 kV and a solid state detector (Rigaku/MS, The Woodlands, TX). A continuous scan was recorded for all samples from 4° to 40° 2 $\theta$  with a step size of 0.02° 2 $\theta$  and a scanning rate of 2°/min.

The variable temperature X-ray powder patterns were obtained using a Bruker AXS D8 Advance diffractometer with CuK $\alpha$  radiation at 40 mA and 40 kV, a position sensitive detector, and hot-stage attachment (Bruker AXS). Data were collected with a continuous scan from 2 $\theta$  4° to 40° at a scan speed of 5°/min using a step size of 0.02°.

### Polarized Microscope

Microscopic analysis was carried out using a Nikon Eclipse E600 Polarized Microscope (Nikon, Tokyo, Japan) equipped with a Spot Insight color digital camera (Diagnostic Instruments, Sterling Heights, MI), supported by Image-Pro<sup>®</sup> Plus 4.1 (Media Cybernetics, Silver Spring, MD).

### Thermal Analysis

A TA Instruments 2920 Differential Scanning Calorimeter (TA Instruments, New Castle, DE)

**Table 1.** Crystal Data and Structure Refinement for Mometasone Furoate Form 1 and the Monohydrate

| Data and Parameter                | Form 1  | Monohydrate   |
|-----------------------------------|---|---|
| Chemical formula                  | C <sub>27</sub> H <sub>30</sub> Cl <sub>2</sub> O <sub>6</sub>  | C <sub>27</sub> H <sub>30</sub> Cl <sub>2</sub> O <sub>6</sub> (H <sub>2</sub> O)   |
| Formula weight                    | 521.41  | 539.43  |
| Temperature                       | 296(2) K  | 296(2) K  |
| Wavelength                        | 0.71073 Å   | 0.71073 Å   |
| Crystal system                    | Orthorhombic  | Triclinic   |
| Space group                       | <i>P</i> 2 <sub>1</sub> 2 <sub>1</sub> 2 <sub>1</sub>   | <i>P</i> 1  |
| Unit cell dimensions              | <i>a</i> = 12.3414(7) Å<br><i>b</i> = 13.5838(7) Å<br><i>c</i> = 14.9376(8) Å<br>$\alpha$ = 90.000(0)°<br>$\beta$ = 90.000(0)°<br>$\gamma$ = 90.000(0)° | <i>a</i> = 7.3208(7) Å,<br><i>b</i> = 8.4767(8) Å<br><i>c</i> = 11.8136(11) Å<br>$\alpha$ = 73.251(2)°<br>$\beta$ = 85.006(2)°<br>$\gamma$ = 69.344(2)° |
| Volume                            | 2504.2(2) Å <sup>3</sup>  | 656.79(11) Å <sup>3</sup>   |
| Z                                 | 4   | 1   |
| Density (calculated)              | 1.383 mg/m <sup>3</sup>   | 1.364 mg/m <sup>3</sup>   |
| Absorption coefficient            | 0.300/mm  | 0.291/mm  |
| F(000)                            | 1096  | 284   |
| Crystal size                      | 1.00 × 0.20 × 0.20 mm <sup>3</sup>  | 0.30 × 0.20 × 0.20 mm <sup>3</sup>  |
| Theta range for data collection   | 2.03–28.26°   | 1.80–28.25°   |
| Index ranges                      | –15 ≤ <i>h</i> ≤ 16<br>–17 ≤ <i>k</i> ≤ 16<br>–15 ≤ <i>l</i> ≤ 19   | –9 ≤ <i>h</i> ≤ 9<br>–6 ≤ <i>k</i> ≤ 11<br>–15 ≤ <i>l</i> ≤ 15  |
| Reflections collected             | 15899   | 4196  |
| Independent reflections           | 5869 [R(int) = 0.1147]  | 3466 [R(int) = 0.0242]  |
| Completeness to theta = 28.26°    | 96.9%   | 90.1%   |
| Absorption correction             | None  | None  |
| Refinement method                 | Full-matrix least-squares on F <sup>2</sup>   | Full-matrix least-squares on F <sup>2</sup>   |
| Data/restraints/parameters        | 5869/0/324  | 3466/3/337  |
| Goodness-of-fit on F <sup>2</sup> | 0.971   | 0.975   |
| Final R indices [I > 2sigma(I)]   | R1 = 0.0531<br>wR2 = 0.1006   | R1 = 0.0342<br>wR2 = 0.0807   |
| R indices (all data)              | R1 = 0.0599<br>wR2 = 0.1041   | R1 = 0.0367<br>wR2 = 0.0822   |

was used to monitor the thermal events as a function of temperature increase. Samples (2–5 mg) in aluminum pans with pin holes were heated from 10 to 300°C at a heating rate of 10°C/min. Thermogravimetric analysis was carried out on a TA Q 500 Thermogravimetric Analyzer (TA Instrument). Samples (5–15 mg) in open pans were heated from 25 to 300°C at 10°C/min, with a nitrogen purge of 100 mL/min.

#### FT-IR Spectroscopy

FT-IR spectra were collected with a resolution of 2.0 cm<sup>–1</sup> using a Nicolet Nexus 670 Bench with Avatar Smart MIRacle ATR, supported with OMNIC 5.2 software (Thermo Electron, Waltham, MA).

#### Dynamic Moisture Adsorption

Water uptake at selected humidity was measured at 25°C using a SGA-100 Symmetric Vapor Sorption Analyzer (VTI, Haileah, FL).

## RESULTS AND DISCUSSION

#### Crystal Structures of Mometasone Furoate Form 1 and its Monohydrate Form

Table 1 provides the details of crystal data collection, structure solution, and structure refinement for both mometasone furoate Form 1 and its monohydrate form. The molecular structure and conformation are shown in Figure 1, with atomic thermal ellipsoids drawn at a 50%

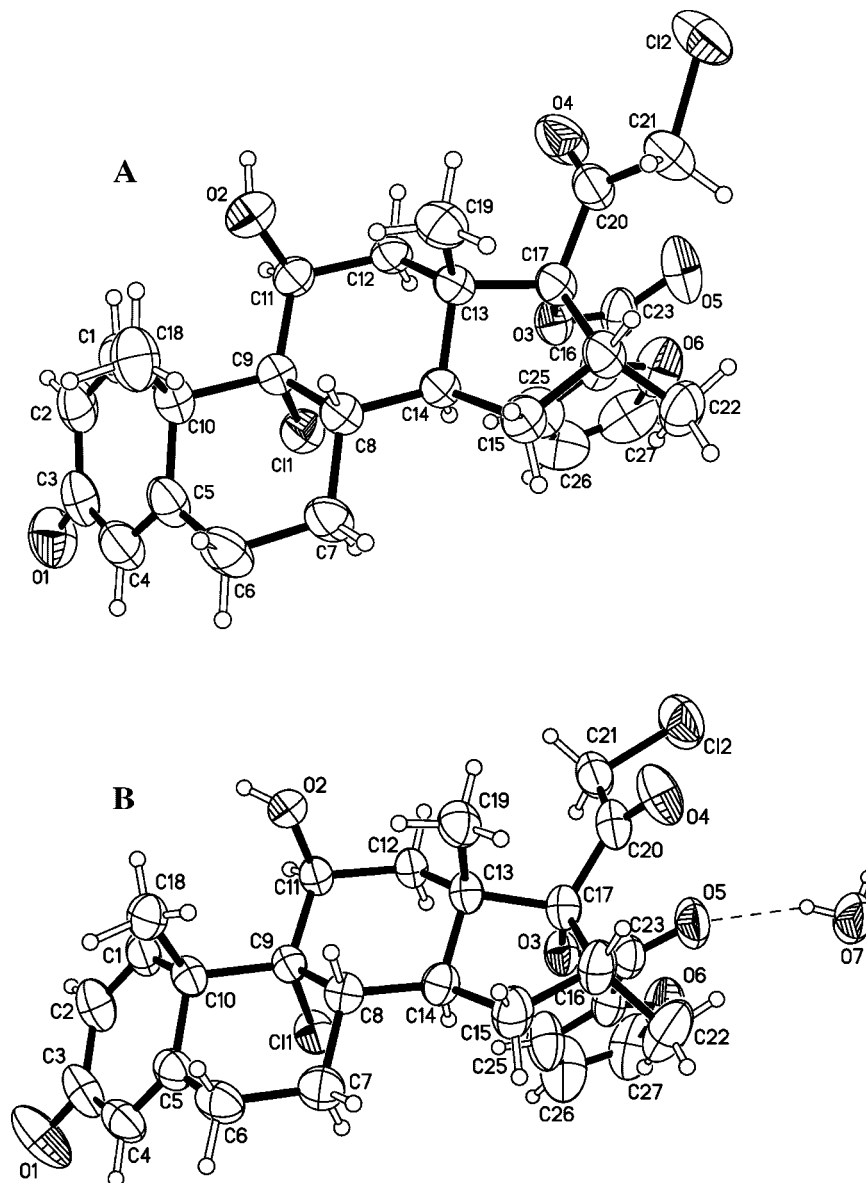


**Figure 1.** The structure of mometasone furoate Form 1 (A) and the monohydrate (B), showing the 50% probability displacement ellipsoids and the atom-numbering scheme.

probability level. The X-ray single crystal analysis agrees with the proposed structure and stereochemistry of the mometasone furoate molecule.<sup>9</sup> Bond lengths and bond angles are in the expected ranges.

For the molecule structure, both forms have similar conformations. The largest difference is in the orientation of the chloroethylone moiety attached to C17. In Form 1 the keto carbonyl oxygen atom at C20 is *cis* to the furoate oxygen atom. In the monohydrate it is *trans* (Tab. 2). Selected bond lengths and angles with the greatest differences are listed in Table 2. For example, the

C(16)-C(22) bond is longer in Form 1 than in the monohydrate, whereas the C(20)-C(21) is longer in the monohydrate. The angle of C(16)-C(17)-C(20) is 5° larger in Form 1 than in the monohydrate.

In Form 1, mometasone furoate crystallizes in the orthorhombic space group,  $P2_12_12_1$ , with  $Z = 4$  (Fig. 2). The cell parameters are  $a = 12.3414(7)$ ,  $b = 13.5838(7)$ ,  $c = 14.9376(8)$  Å,  $\alpha = 90.000(0)^\circ$ ,  $\beta = 90.000(0)^\circ$ ,  $\gamma = 90.000(0)^\circ$  and  $V = 2504.2(2)$  Å<sup>3</sup>. For  $Z = 4$  and  $M = 521.41$ , the calculated density is 1.383 g/cm<sup>3</sup>. A single molecule comprises the asymmetric unit. Thus the mometasone furoate molecules adopt only one conformation in

**Table 2.** Comparison of Selected Bond Distances, Bond Angles, and Torsion Angles in the Crystal Structures of Form 1 and the Monohydrate

| Parameter              | Form 1      | Monohydrate |
|------------------------|-------------|-------------|
| C(16)-C(22)            | 1.527(3) Å  | 1.503(5) Å  |
| C(20)-C(21)            | 1.502(3) Å  | 1.525(4) Å  |
| C(23)-C(24)            | 1.469(4) Å  | 1.449(4) Å  |
| C(9)-C(11)             | 1.543(3) Å  | 1.561(3) Å  |
| C(17)-C(20)            | 1.547(3) Å  | 1.531(4) Å  |
| C(16)-C(17)-C(20)      | 118.29(18)° | 113.6(2)°   |
| C(8)-C(9)-C(11)        | 115.33(16)° | 111.92(18)° |
| O(4)-C(20)-C(21)       | 123.4(2)°   | 120.0(3)°   |
| O(2)-C(11)-C(12)       | 111.72(17)° | 108.98(19)° |
| C(6)-C(7)-C(8)         | 114.45(19)° | 112.1(2)°   |
| C(5)-C(10)-C(18)       | 108.86(19)° | 106.7(2)°   |
| O(3)-C(17)-C(20)-O(4)  | 49.5°       | -143.6°     |
| C(16)-C(17)-C(20)-O(4) | 175.7       | -17.3°      |

Form 1. These molecules are packed tightly and interlocked with one another. Strong intermolecular hydrogen bonding, O(2)-H...O(1)=C, between hydroxyl and ketone groups link neighboring molecules into chains, which propagate along the *a* axis (Tab. 3). Its density of 1.383 g/cm<sup>3</sup> suggests efficient packing.

Mometasone furoate monohydrate has a space group of P1. The triclinic cell parameters are *a* = 7.3208(7), *b* = 8.4767(8), *c* = 11.8136(11) Å,  $\alpha$  = 73.251(2)°,  $\beta$  = 85.006(2)°,  $\gamma$  = 69.344(2)° and *V* = 656.79(11) Å<sup>3</sup>. For *Z* = 1 and *M* = 539.43, the calculated density is 1.364 g/cm<sup>3</sup> (Tab. 1 and Fig. 2). Unlike Form 1, the monohydrate has layered packing with molecules stacked upon each other along the *a* axis. The unit cell contains one molecule of mometasone furoate and one molecule of water. This confirms that the monohydrate is a 1:1 stoichiometric hydrate. The water molecules lie next to the water molecules of the adjoining unit

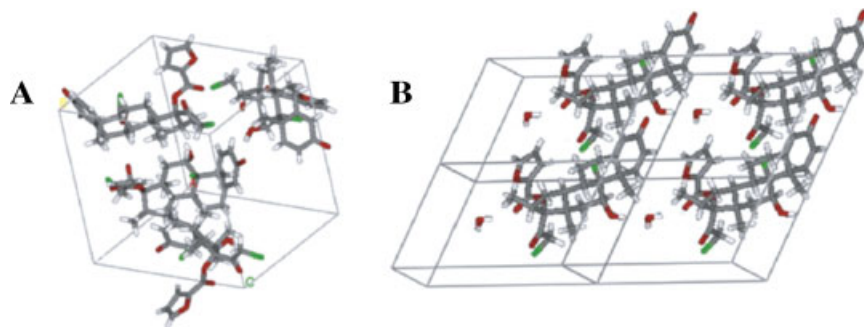
cells along the *a* axis. It can be classified as a channel hydrate.<sup>10</sup> Similar structural characteristics are also present in crystals of ampicillin trihydrate,<sup>11</sup> caffeine hydrate,<sup>12</sup> theophylline hydrate,<sup>13</sup> and thymine hydrate.<sup>14</sup> Each water molecule forms three hydrogen bonds with neighboring mometasone furoate molecules in the crystal structure as listed in Table 3 and illustrated in Scheme 2. There is no hydrogen bonding between mometasone furoate molecules or between water molecules.

### Microscopy

Figure 3 compares the morphology of mometasone furoate Form 1 and the monohydrate form using a polarized light microscope. Both crystalline forms show good birefringence, which indicates that both are highly crystalline material. The morphology is clearly distinct for these materials. Form 1 has acicular morphology. The monohydrate was isolated as platelike crystals. It is obvious that significant preferred orientation will be observed in X-ray powder diffraction due to their needle and platelike morphology.

### X-Ray Powder Diffraction

The experimental X-ray powder diffraction patterns of Form 1 and the monohydrate are compared with their computed patterns from single crystal structures in Figures 4 and 5. The experimental patterns perfectly match the computed patterns. This reveals that the prepared crystalline batches have high phase purity. Distinct differences in the profiles of the two forms are evident. Characteristic diffraction peaks can be observed at 2 $\theta$  values of 9.3, 9.7, 11.3, 13.8, 14.8, 16.0, 18.9, 19.4° for Form 1 and at 2 $\theta$  values

**Figure 2.** Crystal packing of mometasone furoate Form 1 viewed from approximately the 1 1 1 direction (A) and the monohydrate viewed from approximately 1 0 0 direction (B).

**Table 3.** Hydrogen Bond Distances and Angles for Mometasone Furoate Form 1 and the Monohydrate

| Form        | D—H...A                        | D...A (Å) | H...A (Å) | D—H...A (deg) |
|-------------|--------------------------------|-----------|-----------|---------------|
| Form 1      | O(2)—H(2O) (MF1)...O(1)(MF2)   | 2.944     | 1.966     | 163.64        |
| Monohydrate | O(2)—H(2O)(MF1)...O(7)(water)  | 2.732     | 1.928     | 166.56        |
| Monohydrate | O(7)—H(7O2)(water)...O(5)(MF2) | 2.877     | 2.126     | 154.44        |
| Monohydrate | O(7)—H(7O1)(water)...O(1)(MF3) | 2.749     | 1.999     | 152.29        |

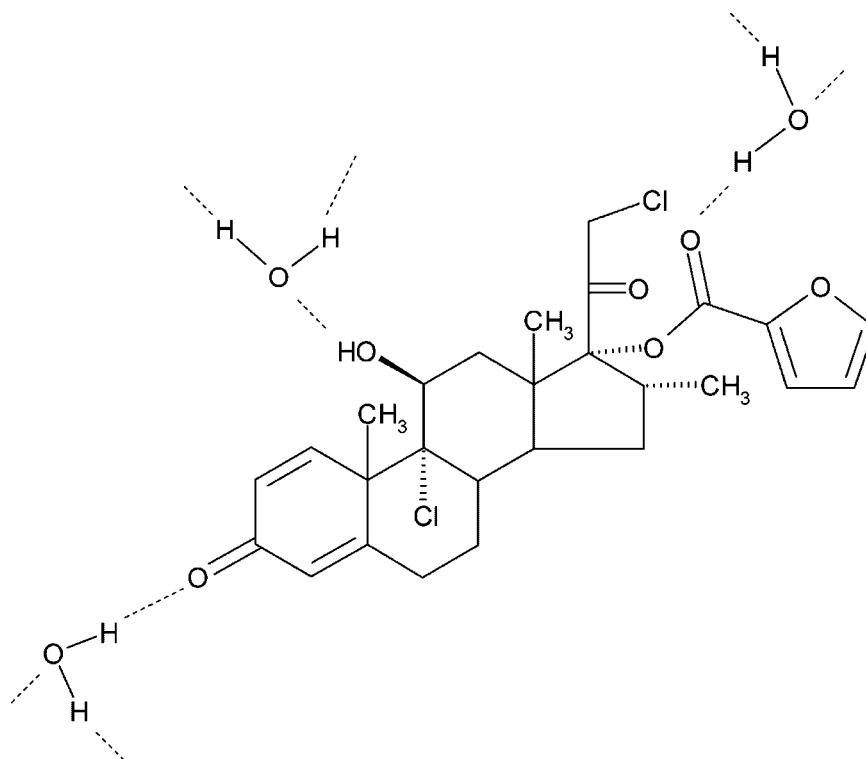
\*MF, mometasone furoate molecule.

of 7.8, 14.0, 15.2, and 18.7° for the monohydrate. These peaks can be used to differentiate these two crystalline forms.

Strong preferred orientation was observed for the unground material. For Form 1, the diffraction peak at  $2\theta$  9.4° is the strongest in the unground sample, which is associated with Miller plane (101) in its crystal structure. It indicates the {101} face is the major face in its acicular crystals. For the unground monohydrate, diffraction peaks at  $2\theta$  7.8, 15.6, and 31.2° are the three most intense peaks. As calculated from the crystal structure, these three peaks are associated with Miller planes (001), (002), (004) respectively. It indicates the major face for the unground monohydrate crystals is {001}.

### Thermal Analysis

Figure 6 illustrates the DSC trace of micronized Form 1 at 10°C/min. There are two overlapping endotherms detected at approximately 233 and 238°C followed by an exotherm at 242°C. Melting of Form 1 was observed in the same temperature range using a hot-stage microscope (data not shown). The complex thermal events around the melting point of Form 1 indicate that mometasone furoate undergoes significant degradation during melting. It agrees with the observed significant weight loss detected over the same temperature range by TGA (Fig. 6). No significant weight loss was observed at lower temperature, which confirms the anhydrous nature of Form 1.



**Scheme 2.** Hydrogen bonding between water and mometasone furoate molecules in the mometasone furoate monohydrate.

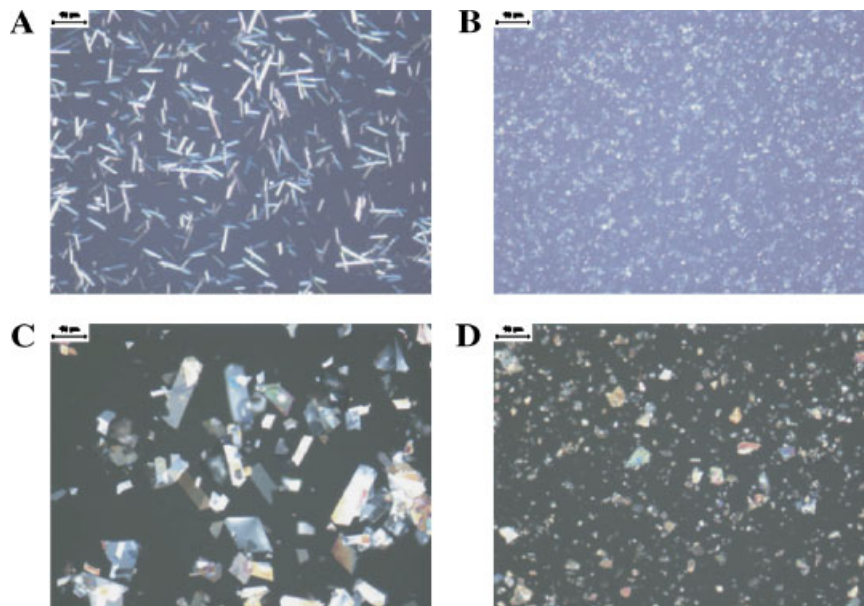


**Figure 3.** Analysis of mometasone furoate anhydrous Form 1 and the monohydrate using a polarized microscope ( $\times 200$ ). (A) Form 1 unground; (B) Form 1 micronized; (C) the monohydrate unground; (D) the monohydrate ground.

For the monohydrate, a broad endothermic peak was observed with an onset temperature of  $64^{\circ}\text{C}$  and peak temperature of  $105^{\circ}\text{C}$  for the unground material (Fig. 6). It is attributed to the dehydration of the monohydrate form. The enthalpy of dehydration is  $89.7 \pm 1.4 \text{ J/g}$ . The 3.2% weight loss observed over the temperature range

of  $70\text{--}120^{\circ}\text{C}$  by TGA (Fig. 6) agrees with the calculated water content of 3.3% for the monohydrate. A small exotherm ( $0.6 \text{ J/g}$ ) was observed between  $180$  and  $200^{\circ}\text{C}$  with onset temperature of  $191^{\circ}\text{C}$  and peak temperature of  $193^{\circ}\text{C}$ , which indicates that there is a phase transition involved in this temperature range. Similar to Form 1, the

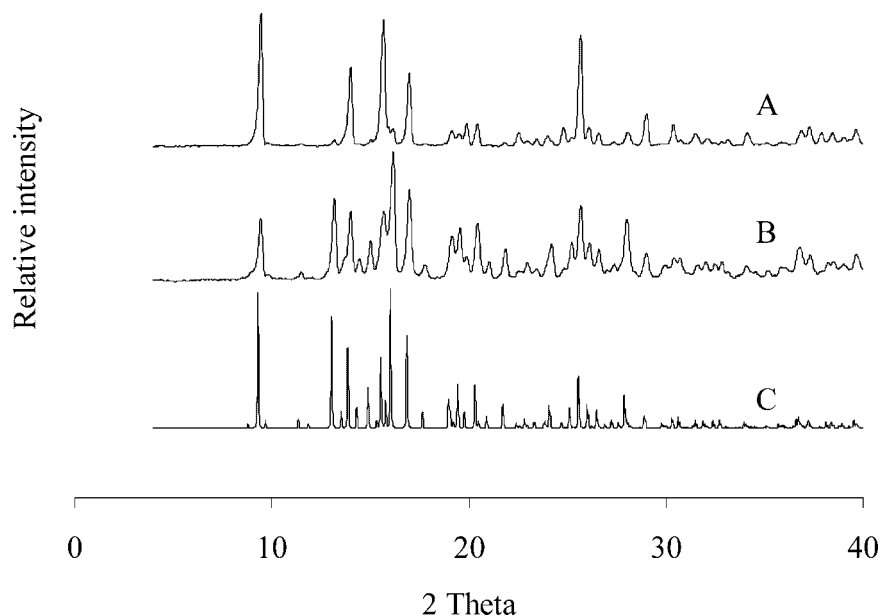


**Figure 4.** X-ray powder pattern of mometasone furoate Form 1. (A) Unground material; (B) micronized material; (C) calculated pattern from the crystal structure.

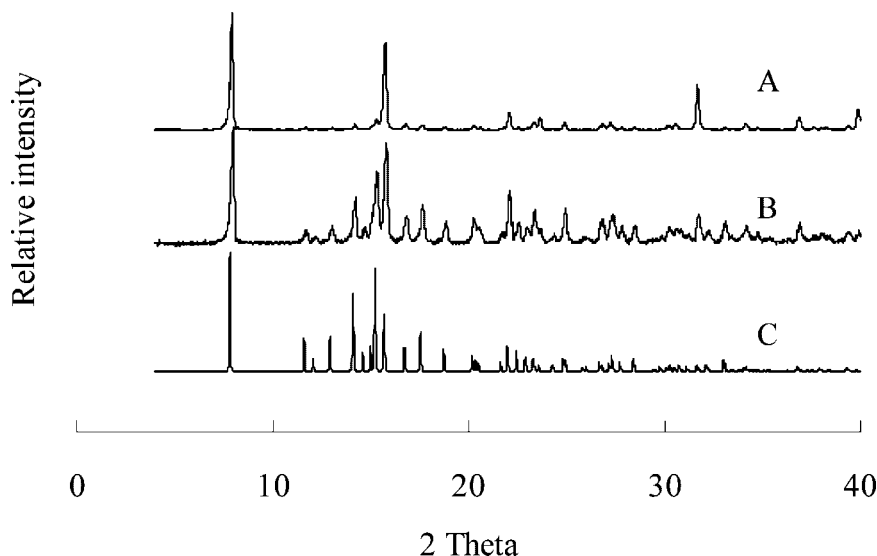


**Figure 5.** X-ray powder pattern of mometasone furoate monohydrate. (A) The unground material; (B) the micronized material; (C) calculated pattern from crystal structure.

endotherms at 233 and 238°C followed by an exotherm at 242°C were due to the melting and degradation of mometasone furoate. A similar thermal profile was observed for the ground material. However, the onset of dehydration is 7–8°C earlier and is due to the kinetic effect of the reduced particle size.

#### FT-IR

Mometasone furoate Form 1 and the monohydrate have distinct FT-IR spectra as shown in Figure 7. The monohydrate form has a broad and weak peak from 3500 to 3600  $\text{cm}^{-1}$ , which is not present in Form 1. It is assumed to be the O-H stretch of water molecules in the crystal lattice. Those characteristic bands reflect “tightly bound” water or crystalline water, which are observed for numerous hydrates.<sup>11,15–17</sup> This is confirmed by the crystal structure of the monohydrate. The water molecule is tightly bound to mometasone furoate molecules with three types of hydrogen bonding.

The three peaks in the carbonyl range from 1650 to 1750  $\text{cm}^{-1}$  reflect the three carbonyl groups in mometasone furoate molecule. Both forms have peaks at 1732 and 1658  $\text{cm}^{-1}$ . However, the carbonyl peak at 1723  $\text{cm}^{-1}$  in Form 1 is shifted to 1706  $\text{cm}^{-1}$  in the monohydrate. It is assigned to the ester carbonyl (C=O(5), Scheme 1), which is not involved in hydrogen bonding in Form 1. Water is hydrogen bonded to that carbonyl in the

monohydrate. Hydrogen bonding weakens the carbonyl bond, resulting in absorption at a lower wavenumber (1706  $\text{cm}^{-1}$ ). The keto carbonyl at position 3 (C=O(1), Scheme 1) is conjugated to two C=C bonds. It is a hydrogen bonding acceptor in both crystalline forms. Resonance and hydrogen bonding weaken the bond, resulting in its absorption at 1658  $\text{cm}^{-1}$  in both forms. The keto carbonyl at position 20 (C=O(4), Scheme 1) absorbs at wavenumber 1732  $\text{cm}^{-1}$  in both forms, indicating the functional group has a similar chemical environment in both crystal structures.

#### Variable Temperature X-Ray Powder Diffraction of Mometasone Furoate Monohydrate

The dehydration process of mometasone furoate monohydrate was investigated using variable temperature X-ray powder diffraction over a temperature range of 30–200°C. As shown in Figure 8, no significant change was observed at 40 and 50°C for the XRPD pattern of the monohydrate. Some characteristic peaks of the monohydrate became broader and had less intensity at 60 and 70°C. At 80°C, those characteristic peaks of the monohydrate significantly decreased in intensity and some new peaks appeared. This indicates that a new crystalline form is produced after dehydration. At 90°C, the peaks of the monohydrate completely disappear and a new crystalline form is observed. The new crystalline form is assumed to be an anhydrous form and named as



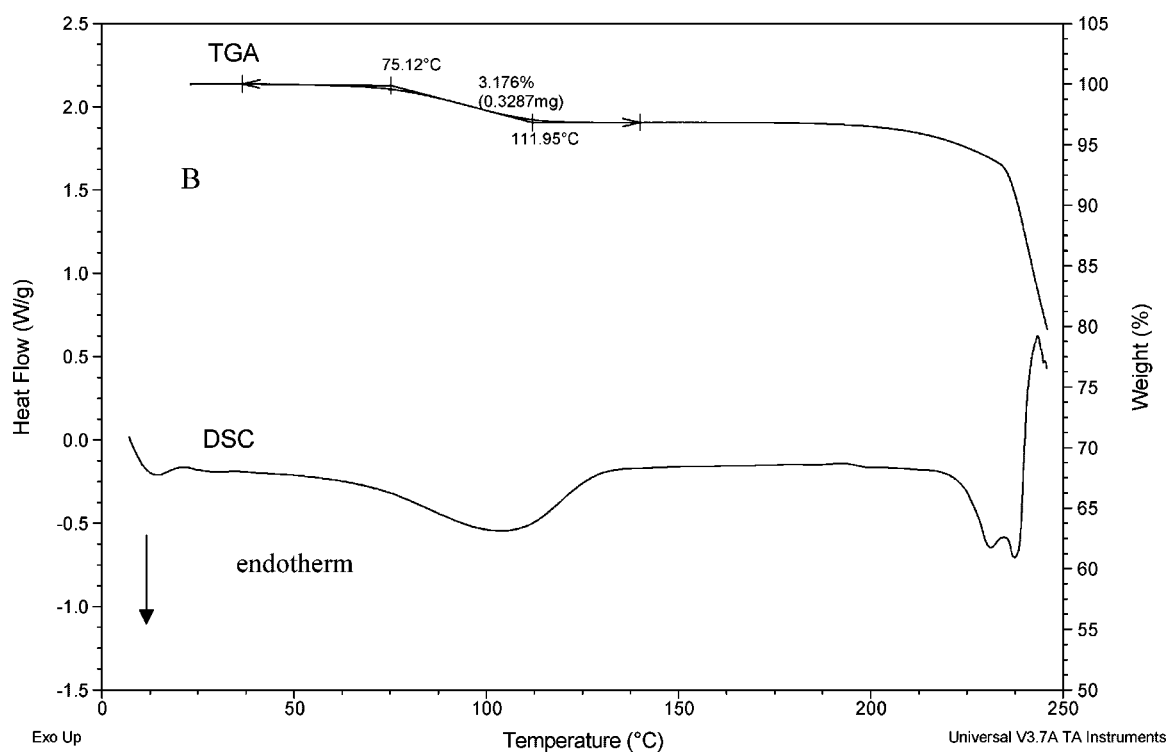
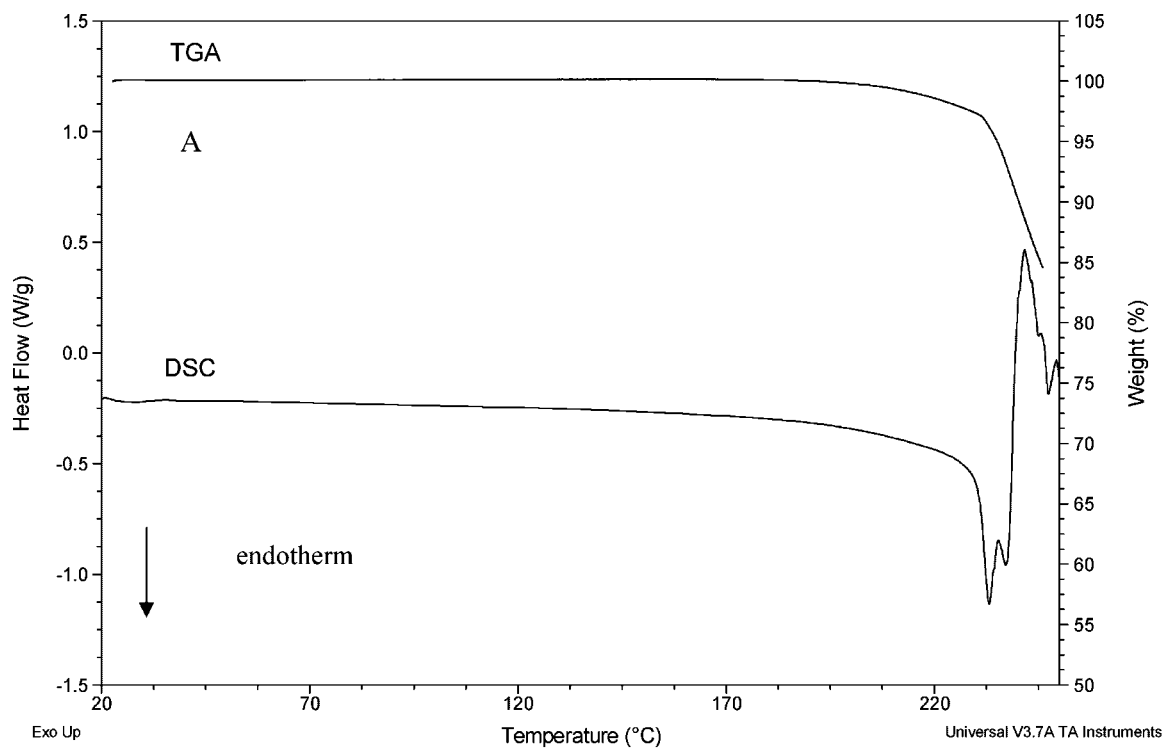


**Figure 6.** DSC and TGA traces of Form 1 (A) and the monohydrate (B) heated at 10°C/min.

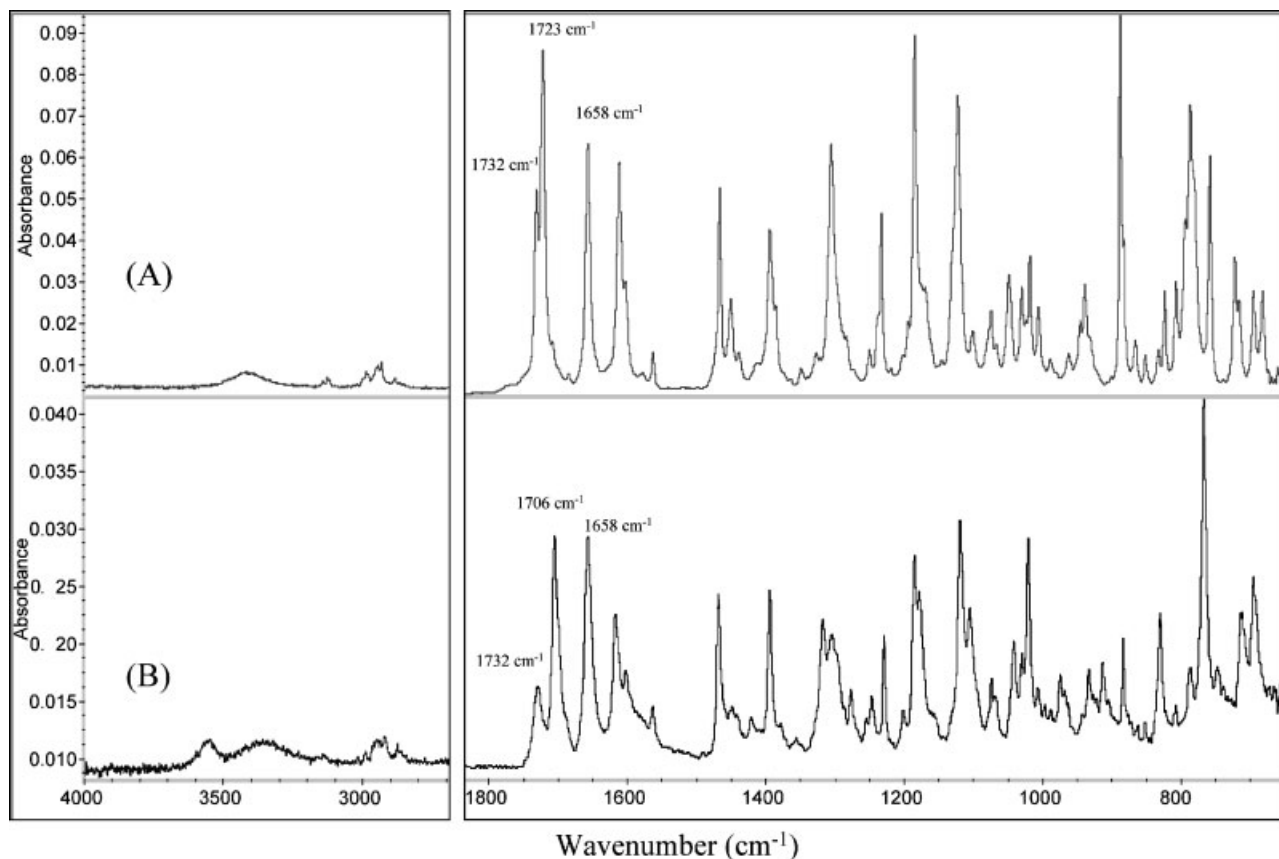


**Figure 7.** FT-IR spectra of mometasone furoate Form 1 (A) and the monohydrate (B).

Form 2. Over the temperature range of 130–200°C, another crystalline form starts to nucleate from Form 2. The intensities of Form 2 peaks decrease and new peaks grow as the temperature increases. The conversion of Form 2 to another anhydrous form is complete at 200°C. The diffraction pattern of this anhydrous form matches the XRPD pattern of Form 1. A small exotherm (0.6 J/g) was observed from 180 to 200°C in DSC, which is probably related to the transition from Form 2 to Form 1.

Form 2 is a metastable anhydrous form. On one hand, it is converted to Form 1 at high temperature. On the other hand, it becomes the monohydrate after cooling to room temperature and being stored under ambient conditions (23°C, 45% RH) as shown in Figure 9. During the variable temperature XRPD investigation, Form 2 was formed above 90°C. After cooling from 120 to 70°C, Form 2 still remains as its original form; however, it is quickly converted to the monohydrate after cooling to room temperature. As shown in Figure 9, characteristic peaks of Form 2 lose

intensity and peaks of the monohydrate appear dramatically. After 1 h at ambient conditions, the XRPD pattern is dominated by the monohydrate form. Overnight, Form 2 completely disappears and the monohydrate is fully formed. The fast conversion of Form 2 to the monohydrate may reflect the similarity of the crystal packing in those two forms. The monohydrate converted from Form 2 has a nearly identical XRPD pattern as the starting material (Fig. 10). This indicates that the process does not introduce significant lattice changes or amorphous content. Interestingly, the unground monohydrate retains its original preferred orientation after being subjected to dehydration to become Form 2, by heating to 120°C, cooling to room temperature, and being kept at ambient conditions overnight (Fig. 10). It reveals that the conversion from the monohydrate to Form 2 or Form 2 back to the monohydrate doesn't involve the random nucleation of the new phases. Rather it is a very ordered process.

As shown in Figure 8, the transformation of Form 2 to Form 1 takes place over a very broad

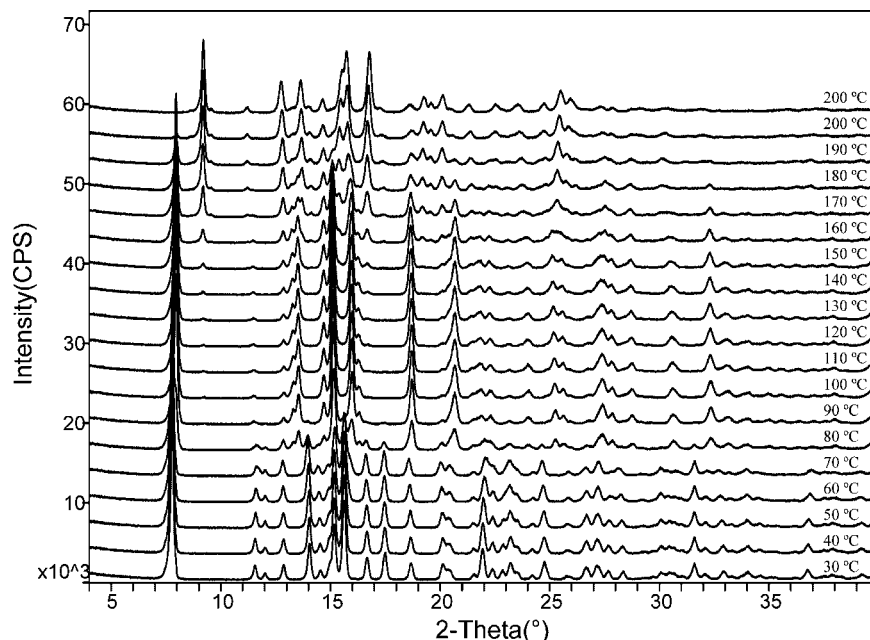


**Figure 8.** Variable temperature X-ray powder diffraction patterns of mometasone furoate monohydrate (ground) heated from 30 to 200°C.

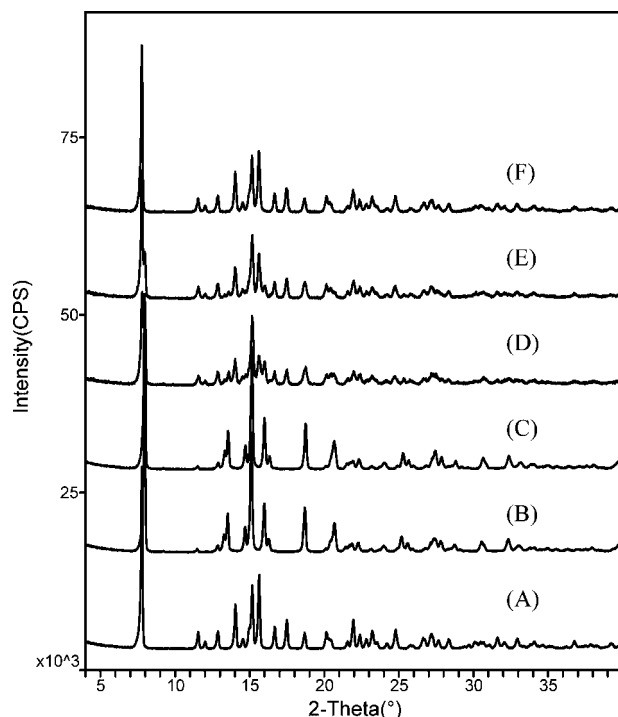


**Figure 9.** Variable temperature X-ray powder pattern of the monohydrate (ground) heated from room temperature (A) to 120°C (B), cooled to 70°C (C), cooled to room temperature with ambient humidity (23°C, 45% RH) (D), at room temperature for 1 h (E), and at room temperature for 24 h (F).

temperature range (150–200°C) and at a very high temperature. It indicates the kinetic barrier of conversion from Form 2 to Form 1. It is probably due to the crystal packing differences of these two crystal forms.

As demonstrated above, the stability order of the monohydrate and Form 2 are determined by both temperature and water activity. At high temperature and low water activity, the monohydrate became metastable and dehydrated, which resulted in the formation of Form 2. After the temperature is lowered to room temperature (23°C), Form 2 is readily hydrated and converted to the monohydrate at ambient humidity (45% RH).

The thermodynamic relationship of Form 1 and the monohydrate are also related to temperature and water activity. It is obvious that Form 1 is more stable than the monohydrate at high temperature and low humidity, because Form 1 is more stable than Form 2 and Form 2 is more stable than monohydrate. On the other hand, Form 1 is 58% more soluble than the monohydrate in water at 40°C (1.50 µg/mL for Form 1 vs. 0.95 µg/mL for the monohydrate). It denotes that the monohydrate is more stable than Form 1 at low temperature and high water activity. However, Form 1 has very good physical stability under humidity. After 3 months at room temperature and 97% RH, no

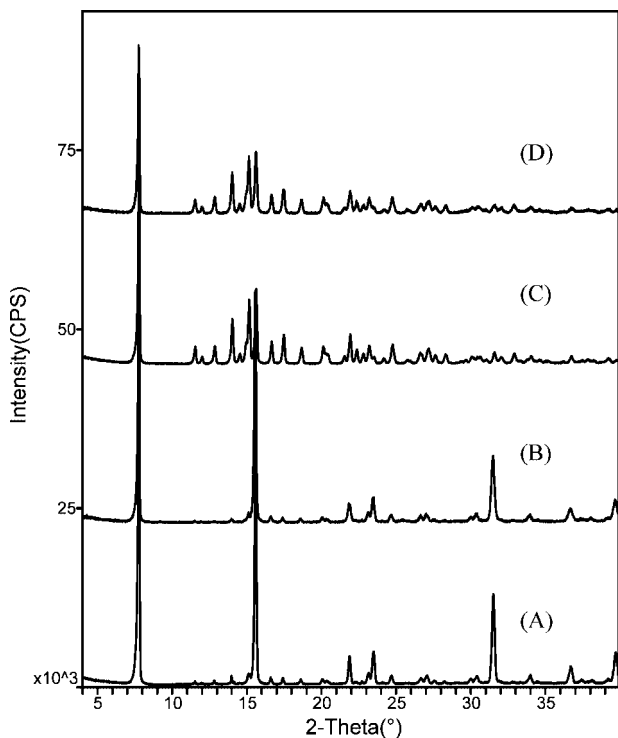


**Figure 10.** X-ray powder of the ground and unground mometasone furoate monohydrate after dehydration and re-hydration. (A) the unground monohydrate; (B) the unground monohydrate after heating to 120°C to become Form 2, cooled to room temperature and kept at ambient conditions for 24 h; (C) the ground monohydrate; (D) the ground monohydrate after the same process of dehydration and re-hydration as the unground material.

conversion to the monohydrate was detected by X-ray powder diffraction (Fig. 11). This can be explained by the distinctly different crystal packing of Form 1 and the monohydrate lattices. It can be envisaged that direct conversion from an interlocked dense packing to a layered structure in the solid state is very difficult. On the other hand, the low solubility of mometasone furoate in water determines that solution-mediated conversion from Form 1 to the monohydrate is negligible.

The thermodynamic order of Form 1 and Form 2 is difficult to investigate at room temperature due to the instability of Form 2. Its instability implies it is meta-stable when compared with Form 1 at room temperature. It is clear that Form 1 is the more stable form at high temperature because Form 2 is converted to Form 1 after heating above 150°C. There is an exotherm observed in the DSC during the transition. Thus, Form 1 and Form 2 are possibly monotropic to each other regarding

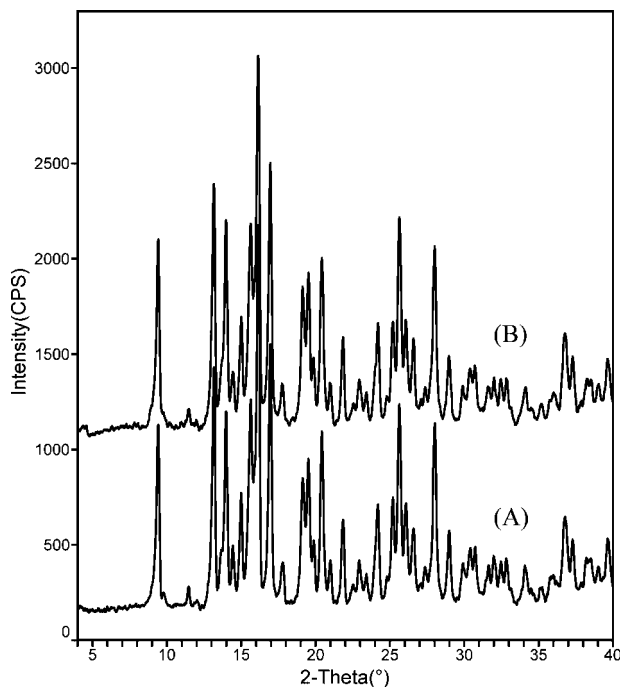


**Figure 11.** X-ray powder diffraction of mometasone furoate Form 1 kept at 23°C, 97% RH. (A) Start; (B) after 3 months at 23°C, 97% RH.

thermodynamic stability according to the Heat of Fusion Rule.<sup>18</sup>

#### Dynamic Moisture Adsorption of Form 1 and Monohydrate

Moisture adsorption of Form 1 and the monohydrate was investigated using the VTI instrument at 25°C. As shown in Figure 12, Form 1 is not hygroscopic and adsorbs only 0.2% moisture at 95% RH. These results confirm that Form 1 has very good physical stability under high humidity and is not converted to the monohydrate form in the solid state. The monohydrate form is also very stable over the humidity range of 5%–95% RH. It adsorbs 0.45% moisture at 95% RH and does not dehydrate significantly at 5% RH and 25°C. However, significant dehydration was observed if the monohydrate was dried at 60°C before moisture adsorption studies. Moreover, the dehydrated material rapidly picks up moisture between 5% and 10% RH, indicating that the dehydrated material is converted back to the monohydrate form easily.

In summary, both Form 1 and the monohydrate have very good physical stability over wide humidity range.

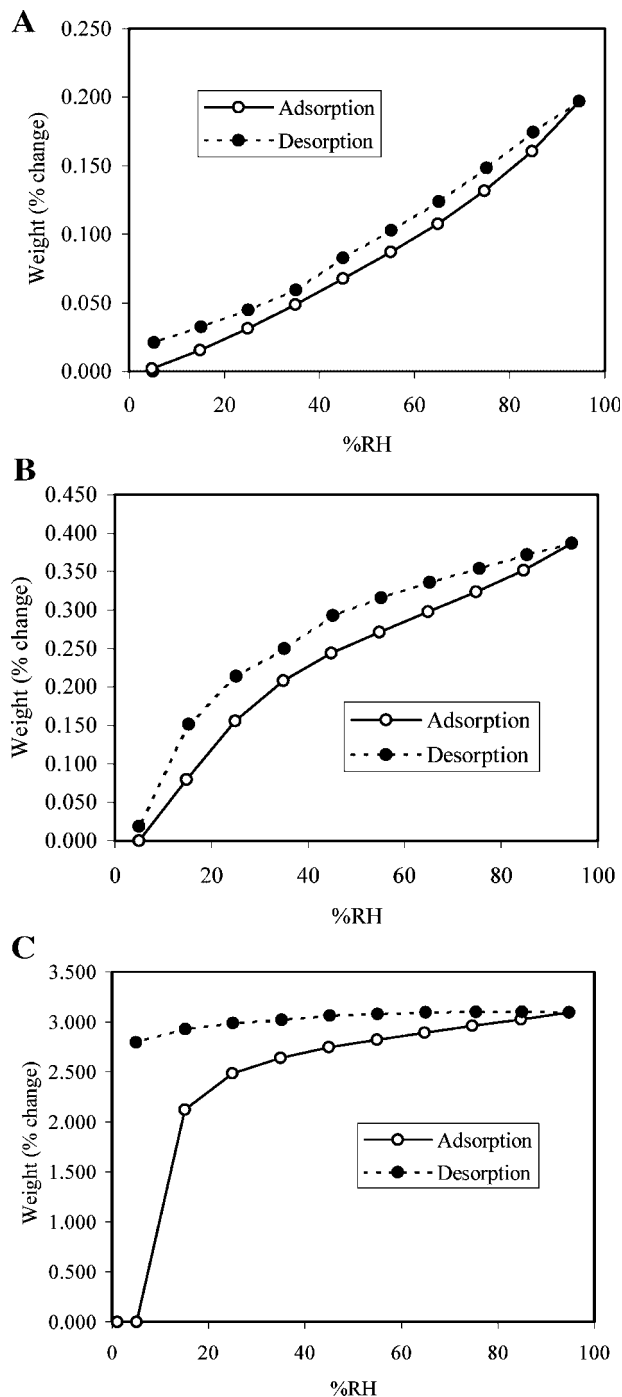


**Figure 12.** Dynamic moisture adsorption of Form 1 and the monohydrate at 25°C. (A) Form 1 with drying; (B) the monohydrate without the drying process; (C) the monohydrate with drying at 60°C.

## CONCLUSIONS

Mometasone furoate anhydrous Form 1 and the monohydrate form have distinct crystal packing even though they have similar molecular con-

formations in their crystal structures. Form 1 has an interlocked crystal structure whereas the monohydrate packs in layers. Water channels exist along the  $a$  axis in the monohydrate. The two forms can be easily differentiated by X-ray powder diffraction and FT-IR. Thermal analysis confirms the anhydrous nature of Form 1. The dehydration process of the monohydrate is clearly illustrated by DSC and TGA analysis. Variable temperature X-ray powder diffraction reveals that the monohydrate is converted to a meta-stable anhydrous form, Form 2, after dehydration. Form 2 is transformed to the stable anhydrous form, Form 1, after being heated above 150°C; and is quickly converted to the monohydrate at 23°C and 45% RH.

## REFERENCES

1. Puar MS, Thompson PA, Ruggeri M, Beiner D, McPhail AT. 1995. An unusual rearrangement product formed during production of mometasone furoate (Sch 32088). *Steroids* 60:612–614.
2. Davies RJ, Nelson HS. 1997. Once-daily mometasone furoate nasal spray: Efficacy and safety of a new intranasal glucocorticoid for allergic rhinitis. *Clini Ther* 19:27–38.
3. Prakash A, Benfield P. 1998. Topical mometasone: A review of its pharmacological properties and therapeutic use in the treatment of dermatological disorders. *Drugs* 55:145–163.
4. Onrust SV, Lamb HM. 1998. Mometasone furoate: A review of its intranasal use in allergic rhinitis. *Drugs* 56:725–745.
5. Berkowitz RB, Bernstein DI, LaForce C, Pedinoff AJ, Rooklin AR, Damaraju CRV, Mesarina-Wicki B, Nolop KB. 1999. Onset of action of mometasone furoate nasal spray (NASONEX®) in seasonal allergic rhinitis. *Allergy* 54:64–69.
6. Sharpe M, Jarvis B. 2001. Inhaled mometasone furoate: A review of its use in adults and adolescents with persistent asthma. *Drugs* 61:1325–1350.
7. Byrn SR, Pfeiffer RP, Stowell JG. 1999. Solid-state chemistry of drugs, 2nd Edition. West Lafayette, Indiana: SSCI, Inc.
8. Yuen PH, Eckhart C, Etlinger T, Levine N. 1992. Preparation and formulation of stable crystalline mometasone furoate monohydrate. *PCT Int Appl* 18: WO 9204365.
9. Shapiro EL, Gentles MJ, Tiberi RL, Popper TL, Berkenkopf J, Lutsky B, Watnick AS. 1987. 17-Heteroaroyl esters of corticosteroids. 2. 11 $\beta$ -hydroxy series. *J Med Chem* 30:1581–1588.
10. Morris KR. 1999. Structural aspects of hydrates and solvates. In: *Polymorphism in pharmaceutical solids*. New York: Marcel Dekker, Inc. 125–181.

11. Brittain HG, Bugay DE, Bogdanowich SJ, DeVincentis J. 1988. Spectral methods for determination of water. *Drug Dev Ind Pharm* 14:2029–2046.
12. Byrn SR, Lin CT. 1976. The effect of crystal packing and defects on desolvation of hydrate crystals of caffeine and L-(–)-1,4-cyclohexandiene-1-alanine. *J Am Chem Soc* 98:4004–4005.
13. Lin CT, Byrn SR. 1979. Desolvations of solvated organic crystals. *Mol Cryst Liq Cryst* 50:99–104.
14. Gerdil R. 1961. The crystal structure of thymine monohydrate. *Acta Crystallogr* 14:333–344.
15. Zhu H, Padden BE, Munson EJ, Grant DJW. 1997. Physicochemical characterization of nedocromil bivalent metal salt hydrates. 2. Nedocromil zinc. *J Pharm Sci* 86:418–429.
16. Bettinetti G, Mura P, Sorrenti M, Faucci MT, Negri A. 1999. Physical characterization of picotamide monohydrate and anhydrous picotamide. *J Pharm Sci* 88:1133–1139.
17. Ledwidge MT, Draper SM, Wilcock DJ, Corrigan OI. 1996. Physicochemical characterization of diclofenac *N*-(2-hydroxyethyl)pyrrolidine: Anhydrate and dihydrate crystalline forms. *J Pharm Sci* 85:16–21.
18. Burger A, Ramberger R. 1979. On the polymorphism of pharmaceuticals and other molecular crystals. II. Applicability of thermodynamic rules. *Mikrochimica Acta* 2:273–316.